Bulletin de la Société Royale des Sciences de Liège, Vol. 87, Actes de colloques, 2018, p. 379 – 386

Properties of Narrow line Seyfert 1 galaxies

Suvendu Rakshit[1]*, Chelliah Subramonian Stalin[1], Hum Chand[2], Xue-Guang Zhang[3]

[1] Indian Institute of Astrophysics, Block II, Koramangala, Bangalore-560034, India
[2] Aryabhatta Research Institute of Observational Sciences (ARIES), 263002, Nainital, India
[3] Institute of Astronomy and Space Science, Sun Yat-Sen University, No. 135, Xingang Xi Road, Guangzhou, 510275, P. R. China

Abstract: Narrow line Seyfert 1 (NLSy1) galaxies constitute a class of active galactic nuclei characterized by the full width at half maximum (FWHM) of the Hβ broad emission line < 2000 km s^{-1} and the flux ratio of [O III] to Hβ < 3. Their properties are not well understood since only a few NLSy1 galaxies were known earlier. We have studied various properties of NLSy1 galaxies using an enlarged sample and compared them with the conventional broad-line Seyfert 1 (BLSy1) galaxies. Both the sample of sources have $z \leq 0.8$ and their optical spectra from SDSS-DR12 that are used to derive various physical parameters have a median signal to noise (S/N) ratio >10 pixel^{-1}. A strong correlation between the Hβ and Hα emission lines is found both in the FWHM and flux. The nuclear continuum luminosity is found to be strongly correlated with the luminosity of Hβ, Hα and [O III] emission lines. The black hole mass in NLSy1 galaxies is lower compared to their broad line counterparts. Compared to BLSy1 galaxies, NLSy1 galaxies have a stronger FeII emission and a higher Eddington ratio that place them in the extreme upper right corner of the $R_{4570} - \lambda_{\rm Edd}$ diagram. The distribution of the radio-loudness parameter (R) in NLSy1 galaxies drops rapidly at $R > 10$ compared to the BLSy1 galaxies that have powerful radio jets. The soft X-ray photon index in NLSy1 galaxies is on average higher (2.9 ± 0.9) than BLSy1 galaxies (2.4 ± 0.8). It is anti-correlated with the Hβ width but correlated with the Fe II strength. NLSy1 galaxies on average have a lower amplitude of optical variability compared to their broad lines counterparts. These results suggest Eddington ratio as the main parameter that drives optical variability in these sources.

1 Introduction

Narrow-line Seyfert 1 (NLSy1) galaxies form a peculiar class of active galactic nuclei (AGNs) that are classified based on their optical emission line properties. They have their full width at half maximum (FWHM) of the Hβ broad emission line < 2000 km s^{-1}, weak [O III] emission lines with a flux ratio of [O III] to Hβ < 3 and strong FeII emission relative to Hβ (Osterbrock & Pogge 1985). They show high amplitude rapid X-ray variability and a strong soft X-ray excess (Boller et al. 1996; Leighly 1999). They harbor low mass black holes ($M_{\rm BH}$, $10^6 - 10^8\,M_\odot$) and have high Eddington ratio (Zhou et al. 2006; Xu et al. 2012; Rakshit et al. 2017a). However, some recent studies suggest

*suvenduat@gmail.com

that NLSy1 galaxies have $M_{\rm BH}$ similar to BLSy1 galaxies and the main difference between them is due to geometrical effects (see Baldi et al. 2016 and references therein).

Although the original definition of NLSy1 galaxies is based on a sharp cutoff in the broad emission line width at 2000 km s^{-1}, there seems to be no such dividing line in the line width distribution of Balmer lines which smoothly merges with the line width distribution of BLSy1 galaxies (Turner et al. 1999). Moreover, some BLSy1 galaxies with Hβ FWHM > 2000 km s^{-1} also exhibit strong Fe II emission and soft X-ray variability (see Grupe et al., 1999). Therefore, studies of various properties of NLSy1 galaxies over a large sample is necessary to understand the similarities and differences of their properties with the conventional BLSy1 galaxies.

In this paper, we present our results on a comparative study of the emission line properties of a sample of NLSy1 and BLSy1 galaxies using a large sample of "QSOs" having a redshift $z < 0.8$ from SDSS-DR12 and discuss their radio, X-ray and optical variability properties. This paper is structured as follows. The spectral analysis is described in Section 2 followed by the optical emission line properties in Section 3. The radio, X-ray and optical variability properties of NLSy1 and BLSy1 galaxies are discussed in Sections 4, 5 and 6, respectively. The conclusions are given in Section 7.

2 Spectral analysis

Recently, Rakshit et al. (2017a) have compiled a new catalog of NLSy1 galaxies consisting of 11,101 objects (a five fold increase from the existing catalog of NLSy1 galaxies, Zhou et al. 2006) after carefully and systematically fitting their continuum and emission line profiles. In addition to NLSy1 galaxies, the spectral fitting process allowed the authors to also obtain a sample of 37,441 BLSy1 galaxies. All the continuum and emission line information obtained from their analysis is used here.

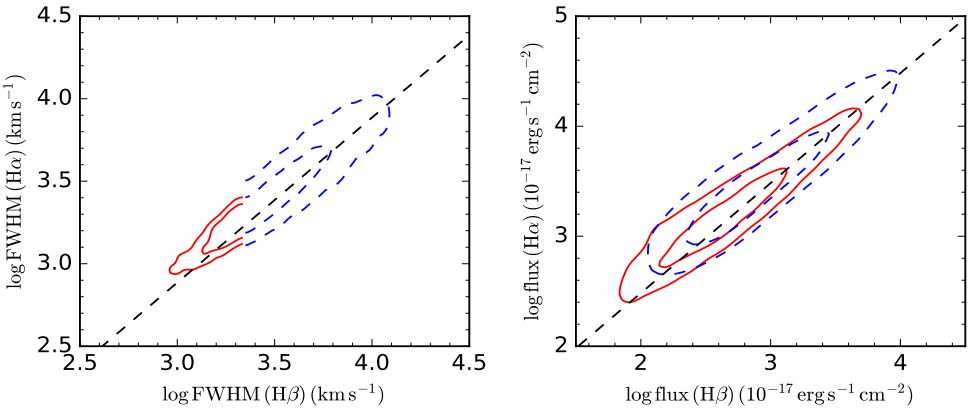

Figure 1: Left: Plot of FWHM(Hα) against FWHM(Hβ) for NLSy1 galaxies (solid red contours) and BLSy1 galaxies (dashed blue contours). Right: Flux (Hα) plotted against flux (Hβ). The dashed black line is the least squares fit to the data. The 68 percentile (inner) and 95 percentile (outer) density contours are shown in each panel.

The detailed spectral fitting procedure is described in Rakshit et al. (2017a). However, we summarize them briefly below. SDSS-DR12 spectra were obtained for all the objects classified as "QSOs" by the SDSS-DR12 pipeline and having $z < 0.8$. This gave 114,806 objects out of which many objects have a poor S/N ratio. Objects with a median S/N $> 2\,{\rm pixel}^{-1}$ were considered for further analysis which resulted in 68,859 sources. Systematic spectral fitting was done on these sources via a two step process:

1. **Host galaxy decomposition:** The optical spectrum of low redshift AGNs will have significant contribution from their host galaxy star light, and therefore to properly analyse their emission line properties, one needs to remove the star light contribution. The continuum of each of the SDSS spectrum was therefore fitted using two components; (i) a power law AGN component and (ii) a stellar contribution from the host galaxy. AGN emission lines were masked except the Fe II multiplets during the fitting. Simple Stellar Population (SSP) templates from Bruzual & Charlot (2003) were used to model the host contribution in the SDSS spectra. A total of 39 templates having ages $5 - 12$Gyr and solar metallicities $Z = 0.008$, 0.05 and 0.02 were used. The AGN continuum was modeled as a power law. The continuum fitting was performed using the Levenberg-Marquardt least-squares minimization implemented in the IDL routine "mpfit" fitting package allowing us to decompose the host contribution from SDSS spectra. We then removed the stellar contribution leaving only the AGN contribution.

2. **Emission line fitting:** After removing the stellar contribution from the SDSS spectra, several lines in the Hβ and Hα regions were fitted along with a FeII template from Kovacevic et al. (2010) and the local AGN continuum with a power law (around the Hβ and Hα regions). The lines fitted in the Hβ region are broad and narrow components of Hβ, He II$\lambda 4687\AA$ and [O III]$\lambda 4959, 5007\AA$ doublet while those in the Hα region are broad and narrow Hα, [O I]$\lambda 6300, 6363\AA$, narrow [N II]$\lambda 6548, 6583\AA$ doublet and the narrow [S II]$\lambda 6716, 6731\AA$. Both the Hα and Hβ regions were fitted simultaneously for objects having $z < 0.3629$.

Though our initial sample was the result of fitting all spectra with a median S/N > 2 pixel^{-1}, in this work, we consider only those objects having a median S/N > 10 pixel^{-1} and the Fe II strength (R_{4570}; ratio of Fe II line flux in the wavelength range $4434 - 4684$ Å to Hβ flux) > 0.01. This S/N cut is imposed so as to have unambiguous estimate of the emission line parameters. This yielded 4070 NLSy1 and 14,314 BLSy1 galaxies, which form the sample analysed in this work.

3 Emission line properties

To study the emission line properties we have plotted in Fig. 1 the FWHM(Hα) against FWHM(Hβ) on the left panel both for NLSy1 (red contours) and BLSy1 galaxies (blue dashed contours). The 68 percentile (inner) and 95 percentile (outer) density contours are shown. A least squares fit of the full sample yields $\mathrm{FWHM(H}\alpha) = (0.768 \pm 0.004) \times \mathrm{FWHM(H}\beta)$ suggesting a strong correlation between the two parameters. On the right panel, we have plotted the flux(Hα) against the flux(Hβ). A least squares fit gives the relation: $\mathrm{flux(H}\alpha) = (3.09 \pm 0.01) \times \mathrm{flux(H}\beta)$. These relations are consistent with the finding of Zhou et al. (2006) and others.

In Fig. 2, we have plotted the luminosity of several emission lines against the monochromatic nuclear continuum luminosity (λL_{5100}). Luminosity of Hβ (left), Hα (middle) and [O III] (right) is plotted against λL_{5100}. All the correlations are very strong which remain valid even if we divide the entire sample into smaller redshift bins. Linear least squares fits yield

$$\log(L_{\mathrm{H}\beta}) = (1.217 \pm 0.003) \times \log(\lambda L_{5100}) + (-11.43 \pm 0.13) \quad (1)$$

$$\log(L_{\mathrm{H}\alpha}) = (1.148 \pm 0.006) \times \log(\lambda L_{5100}) + (-7.87 \pm 0.26) \quad (2)$$

$$\log(L_{[\mathrm{OIII}]}) = (0.880 \pm 0.005) \times \log(\lambda L_{5100}) + (2.84 \pm 0.22) \quad (3)$$

These results are consistent with the relation found by June et al. (2015). According to June et al. (2015), the relation between line and continuum luminosity is valid over a wide luminosity and redshift ($z = 0 - 6$) ranges. This means that the response of the gas clouds in the broad line

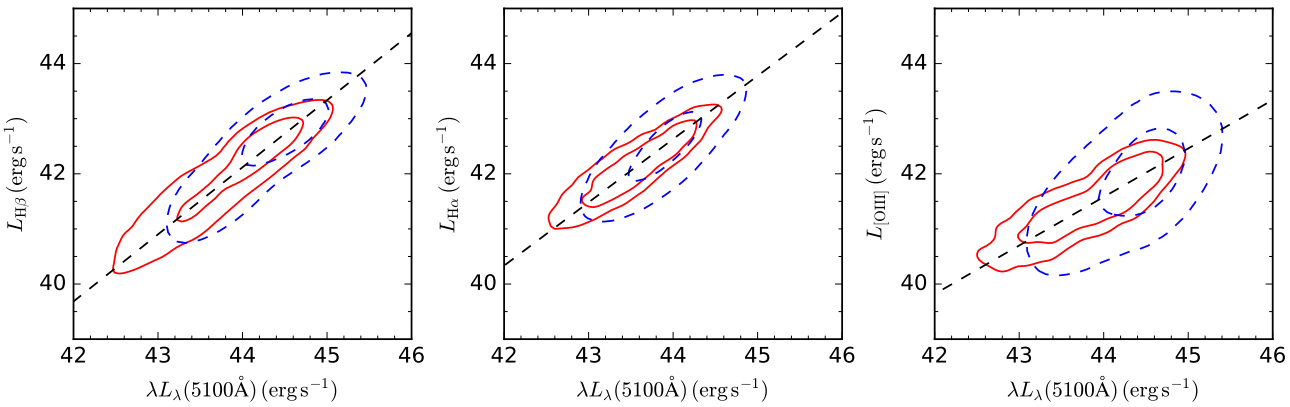

Figure 2: From left to right, the luminosity of Hβ, Hα and [O III] (λ5007Å) plotted against the monochromatic luminosity at 5100 Å for NLSy1 galaxies (solid red contours) and BLSy1 galaxies (dashed blue contours). The dashed black line is the linear fit to the data considering all objects. The 68 percentile (inner) and 95 percentile (outer) density contours are shown in each panel.

region (BLR) to the incident ionizing continuum is the same over a wide redshift range. Such strong correlations between the line and the continuum luminosity have a significant implication on ($M_{\rm BH}$) measurements in AGN using the virial relation. In some AGNs where the host galaxy contamination is large and the emission from the relativistic jet is significant, estimation of the continuum luminosity would be difficult and thus the emission line luminosity could be used as a surrogate for the continuum luminosity. Hence, the correlation between the luminosity of [O III] and λL_{5100} is crucial as it can be used to estimate the bolometric luminosity and $M_{\rm BH}$ in Seyfert 2 AGNs. The $M_{\rm BH}$ values for all objects were estimated using the virial relationship given as

$$M_{\rm BH} = f\frac{R_{\rm BLR}\Delta v^2}{G} \tag{4}$$

where f is an unknown geometrical factor that depends on the BLR geometry and kinematics (see Rakshit et al. 2015 and the references therein), Δv is the FWHM of the broad emission line and $R_{\rm BLR}$ is the radius of the BLR estimated using the reverberation mapping scaling relation (Bentz et al. 2013)

$$\log R_{\rm BLR}({\rm lt-day}) = 1.527 + 0.533 \times \log\left(\frac{\lambda L_\lambda(5100\text{Å})}{10^{44}}\mathrm{erg\,s^{-1}}\right). \tag{5}$$

We used $f = 0.75$ considering a spherical distribution of clouds and estimated $M_{\rm BH}$. We also calculated the Eddington ratio (ξ_λ), which is defined as $\xi_\lambda = L_{\rm bol}/L_{\rm Edd}$ where $L_{\rm bol} = 9 \times \lambda L_\lambda(5100)$ (Kaspi et al. 2000) and $L_{\rm Edd} = 1.3 \times 10^{38} M_{\rm BH}/M_\odot$ erg s^{-1}.

We show in Fig. 3, the variation of R_{4570} against $M_{\rm BH}$ (left panel) and the Eddington ratio (right panel) for both NLSy1 and BLSy1 galaxies. The 68 percentile (inner) and 95 percentile (outer) density contours are also shown in each panel. It is clear from Fig. 3 that NLSy1 galaxies occupy a unique location in the $R_{4570} - M_{\rm BH}$ and $R_{4570} - \xi_{\rm Edd}$ plane. They have a lower black hole mass, higher Fe II strength and higher Eddington ratio compared to their broad line counterparts. Thus, in the $R_{4570} - M_{\rm BH}$ diagram, NLSy1 galaxies are situated at the extreme top left while in the $R_{4570} - \xi_{\rm Edd}$ diagram their location is at the top right corner. Thus, one can use the $R_{4570} - M_{\rm BH}$ and $R_{4570} - \xi_{\rm Edd}$ diagrams to distinguish between NLSy1 and BLSy1 galaxies.

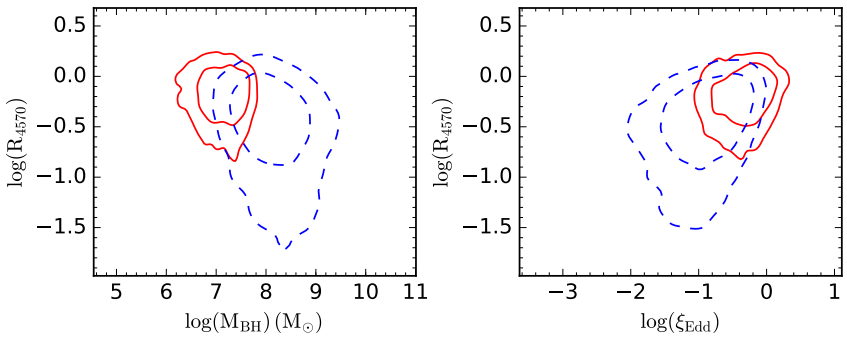

Figure 3: The relation between R_{4570} and black hole mass (left) and Eddington ratio (right) for NLSy1 galaxies (solid red contours) and BLSy1 galaxies (dashed blue contours). The 68 percentile (inner) and 95 percentile (outer) density contours are shown in each panel.

4 Radio properties

BLSy1 galaxies usually show stronger radio emission than NLSy1 galaxies (Komossa et al. 2006). In Rakshit et al. (2017a) we found that about 5% of the NLSy1 galaxies have been detected in the FIRST survey within a search radius of 2″. Among the sources studied in this work, 383 NLSy1 galaxies and 1547 BLSy1 galaxies have been detected by FIRST. We calculated their radio loudness parameter (R) using $R = F_{1.4\mathrm{GHz}}/F_g$, where $F_{1.4\mathrm{GHz}}$ is the 1.4GHz radio flux density and F_g is the flux density in the optical g-band. Their radio loudness distribution is plotted in the left panel of Fig. 4. We found that the R distribution in the case of NLSy1 drops much rapidly after $R \sim 10$ compared to BLSy1 galaxies. Both the distributions however peak at $R \sim 10$. The radio power ($P_{1.4GHz}$) was calculated following Rakshit et al. (2017a) and plotted in the right panel of Fig. 4. The histograms clearly show that BLSy1 galaxies have powerful jets compared to NLSy1 galaxies.

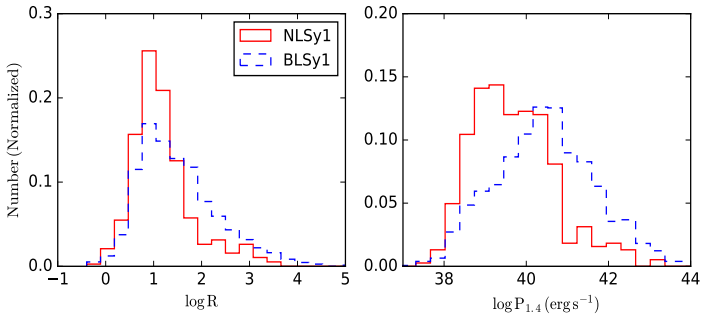

Figure 4: The distribution of radio loudness (left) and radio power (right) for NLSy1 (solid-line) and BLSy1 (dashed-line) galaxies.

5 X-ray properties

One of the important characteristics of NLSy1 galaxies is that they exhibit rapid X-ray variability and have soft X-ray spectra (see Boller et al. 1996; Leighly 1999). To study the X-ray properties of the objects in our sample we looked for their X-ray counterparts in the ROSAT all-sky survey (2RXS) source catalog (Boller et al. 2016) within a search radius of 30″ (see Rakshit et al. 2017a for more

details). We found that about 1300 NLSy1 and 3600 BLSy1 galaxies in our sample studied here have X-ray counterparts in ROSAT. We plotted their soft X-ray (0.1−2 keV) flux in the first panel of Fig. 5. Both the distribution of soft X-ray flux for NLSy1 and BLSy1 galaxies are similar. The distribution of their photon indices taken from the 2RXS catalog is shown in the second panel. The photon index distribution has a median value of $\Gamma = 2.9 \pm 0.9$ for NLSy1 galaxies and $\Gamma = 2.4 \pm 0.8$ for BLSy1 galaxies suggesting that NLSy1 galaxies on average have a steeper soft X-ray spectrum than BLSy1 galaxies. This result from an analysis of a large sample of objects is consistent with the findings of Leighly (1999). In the third panel of Fig. 5, Γ is plotted against the width of the Hβ broad component for NLSy1 and BLSy1 galaxies. We found that Γ is anti-correlated with the Hβ width suggesting that the NLSy1 galaxies have Γ larger than BLSy1 galaxies. The Spearman rank correlation gives a value of -0.32 suggesting a moderate anti-correlation between the two parameters. In the last panel, Γ is plotted against R_{4570}. We find a weaker but positive correlation between the two having a Spearman rank correlation coefficient of 0.21 suggesting that strong Fe II emitters have a higher Γ, which is larger for NLSy1 galaxies than for BLSy1 galaxies.

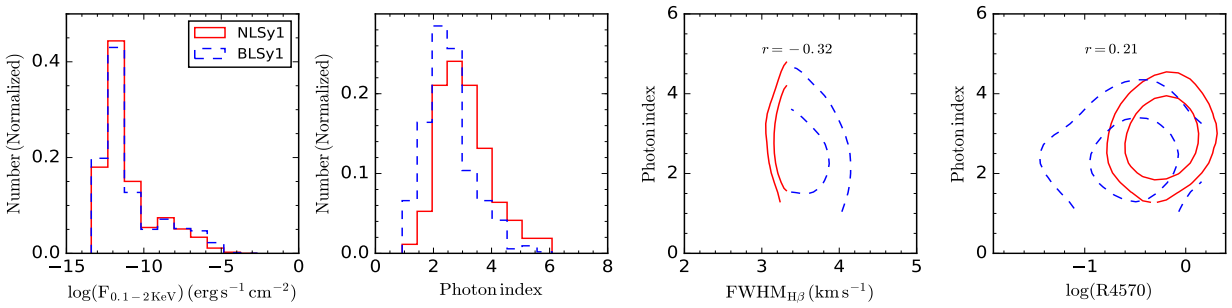

Figure 5: From left to right the distribution of the soft X-ray (0.1−2 keV) flux, the distribution of the photon index, the variation of the photon index with the FWHM of the Hβ broad component, and the variation of the photon index with R_{4570} is plotted. The Spearman rank correlation coefficients are given in each panel. The 68 percentile (inner) and 95 percentile (outer) density contours are shown in the third and fourth panels.

6 Optical variability properties

AGNs are known to show rapid variability across all wavelengths over time scales of days to years. However, the origin of such variations is poorly understood. To understand this, several studies have been conducted using a large sample of Seyfert 1 galaxies. The amplitude of the optical variability is found to be correlated with several observables such as wavelength, luminosity, redshift, $M_{\rm BH}$ and Eddington ratio (see MacLeod et al. 2010 and references therein). However, studies on the optical variability of NLSy1 galaxies are very limited. Klimek et al. (2004) and more recently Ai et al. (2010,2013) have performed an optical variability study of a small sample of NLSy1 galaxies and found that they are less variable than BLSy1 galaxies. As NLSy1 galaxies have a low $M_{\rm BH}$ and a high Eddington ratio, variability studies of NLSy1 galaxies along with BLSy1 galaxies will enable one to probe the variability characteristics of AGNs over a wide range of $M_{\rm BH}$ and Eddington ratio.

Using the extended NLSy1 galaxies catalog of Rakshit et al. (2017a), we have recently performed a comparative study of the optical variability of a large sample of NLSy1 and BLSy1 galaxies matched in luminosity and redshift (Rakshit et al. 2017b). For this purpose, we used the optical V-band light curves from the Catalina Real Time Transient Survey (CRTS) covering more than 5 years of

observation and having a minimum of 50 photometric data points in each light curve. The light curves were modeled using the JAVELIN code which uses a damped random walk model (see Zu et al., 2011 and references therein) allowing to estimate the amplitude of variability (σ_d) of all the BLSy1 and NLSy1 galaxies. In addition, the intrinsic amplitude of variability (σ_m) was estimated from the measured variance of the observed light curves after subtracting the measurement errors. The σ_d calculated using JAVELIN is found to be consistent with the value of σ_m (see Rakshit et al., 2017b). The optical variability amplitude is found to be lower in NLSy1 galaxies compared to BLSy1 galaxies. In Fig. 6, we show the dependency of the amplitude of variability with R_{4570} and $\xi_{\rm Edd}$ in the left and middle panels. The amplitude of variability is anti-correlated with both R_{4570} and $\xi_{\rm Edd}$. The right panel shows the distribution of amplitude of variability for NLSy1 and BLSy1 galaxies clearly stating that on average NLSy1 galaxies are less variable in the optical band than BLSy1 galaxies. As R_{4570} and the Eddington ratio are strongly correlated it is likely that the difference in the variability between NLSy1 and BLSy1 galaxies might be in part due to differences in the Eddington ratio between them. To investigate this, we created a subsample of NLSy1 and BLSy1 galaxies matched in Eddington ratio. In this subsample, we find no difference in variability between BLSy1 and NLSy1 galaxies, thereby, suggesting the Eddington ratio as the most fundamental parameter driving optical variabiltiy. More details can be found in Rakshit et al. (2017b).

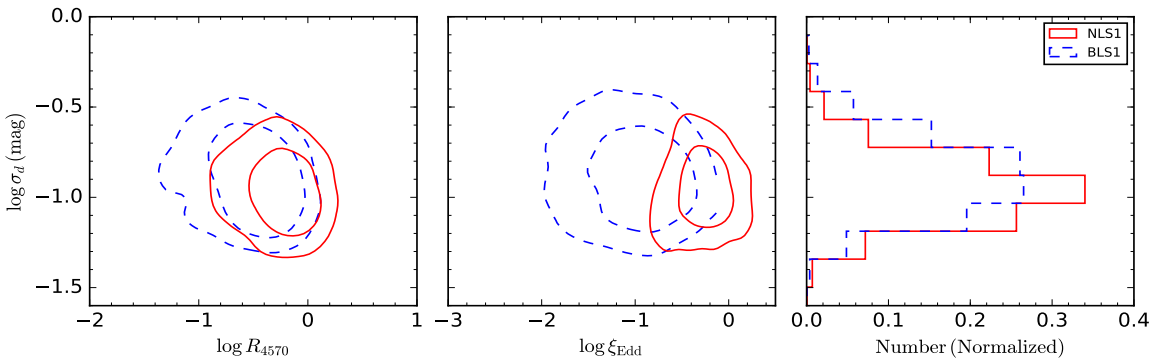

Figure 6: Density contours of the amplitude of variability against R_{4570} (left) and $\xi_{\rm Edd}$ (middle) for 68 (inner) and 95 percentile (outer) of the sample. The right panel shows the distribution of the amplitude of variability for NLSy1 and BLSy1 galaxies. Figure adapted from Rakshit et al. (2017b).

7 Conclusion

We have studied the emission line and variability properties of a large sample of NLSy1 and BLSy1 galaxies from SDSS-DR12. The emission line parameters were taken from the work of Rakshit et al. (2017a). Our sample consists of 4070 NLSy1 and 14,314 BLSy1 galaxies having a median S/N $> 10\,{\rm pixel}^{-1}$ and $R_{4570} > 0.01$. The results of this work are summarized below.

1. The line widths of Hβ and Hα are strongly correlated via the relation ${\rm FWHM(H}\alpha) = (0.768 \pm 0.004) \times {\rm FWHM(H}\beta)$ for the entire sample. Also, a strong correlation is found between the fluxes of Hα and Hβ lines in both NLSy1 and BLSy1 galaxies. For the combined sample we find ${\rm flux(H}\alpha) = (3.09 \pm 0.01) \times {\rm flux(H}\beta)$.

2. The luminosity of the Balmer lines as well as [O III] is found to be strongly correlated with the continuum luminosity at 5100 Å. This suggests that the response of the BLR on the ionizing continuum is identical over a wide range of redshift and luminosity.

3. NLSy1 galaxies have a higher Fe II strength, lower $M_{\rm BH}$ and higher Eddington ratio compared to BLSy1 galaxies. These characteristics place them at the extreme top left corner in the $R_{4570} - M_{\rm BH}$ and top right corner in the $R_{4570} - \xi_{\rm Edd}$ diagrams.

4. The radio loudness distribution of both the NLSy1 and BLSy1 galaxies peaks at about R = 10 but drops rapidly after $R \sim 10$ for NLSy1 compared to BLSy1 galaxies. The latter show more powerful jets compared to the former.

5. NLSy1 galaxies on average have a higher photon index (Γ = 2.9 ± 0.9) or steeper soft X-ray spectrum compared to the BLSy1 galaxies which have a Γ of 2.4 ± 0.8. A moderate anti-correlation between Γ and the width of the emission line is found considering the whole sample. The photon index is positively correlated with the R_{4570}.

6. NLSy1 galaxies on average have a lower amplitude of variability compared to the BLSy1 galaxies and it is anti-correlated with the R_{4570} and $\xi_{\rm Edd}$. Our analysis indicates that the $\xi_{\rm Edd}$ plays an important role in driving optical flux variations in AGNs.

Acknowledgements

We are grateful to the anonymous referee and Jean Surdej (guest co-editor) for their suggestions on our manuscript. We are thankful to the organizers of "The First BINA Workshop" in ARIES, Nainital, India for providing an opportunity to present our work. S.R. thanks Neha Sharma for carefully reading the manuscript.

References

Ai Y. L., Yuan W., Zhou H. Y. et al. 2010, ApJL, 716, L31
Ai Y. L., Yuan W., Zhou H. Y. et al. 2013, AJ, 145, 90
Baldi R. D., Capetti A., Robinson A. et al. 2016, MNRAS, 458, 69
Bentz M. C., Denney K. D., Grier C. J. et al. 2013, ApJ, 767, 149
Boller T., Brandt W. N., Fink H. 1996, A&A, 305, 53
Boller T., Freyberg M. J., Trumper J. et al. 2016, A&A, 588, 103
Bruzual G., Charlot S. 2003, MNRAS, 344, 1000
Grupe D., Beuermann K., Mannheim K., Thomas H.-C. 1999, A&A, 350, 805
Jun H. D., Im M., Lee H. M. et al. 2015, ApJ, 806, 109
Kaspi S., Smith P. S., Netzer H. et al. 2000, ApJ, 533, 631
Kauffmann G., Heckman T. M., Tremonti C. et al. 2003, MNRAS, 346, 1055
Klimek E. S., Gaskell C.M., Hedrick C. H. 2004, ApJ, 609, 69
Komossa S., Voges W., Xu D. et al. 2006, AJ, 132, 531
Kovacevic J., Popovic L. C., Dimitrijevic M. S. 2010, ApJS, 189, 15
Leighly K. M. 1999, ApJS, 125, 317
MacLeod C. L., Ivezic Z., Kochanek C. S. et al. 2010, ApJ, 721, 1014
Osterbrock D. E., Pogge R. W. 1985, ApJ, 297, 166
Rakshit S., Stalin C. S. 2017, ApJ, 842, 96
Rakshit S., Petrov R. G., Meilland A., Honig S. F. 2015, MNRAS, 447, 2420
Rakshit S., Stalin C. S., Chand H. et al. 2017, ApJS, 229, 2
Turner T. J., George I. M., Nandra K. et al. 1999, ApJ, 524, 667
Xu D., Komossa S., Zhou H. et al. 2012, AJ, 143, 83
Zhou H., Wang T., Yuan W. et al. 2006, ApJS, 166, 128
Zu Y., Kochanek C. S., Peterson B. M. 2011, ApJ, 735, 80